Gas mixture component analysis based on array of air-filled quartz capillary-attached metal oxide semiconductor gas sensors

B. BAHRAMINEJAD[a*], S. NOR BASRI[b]
[a]*Department of electrical engineering, Faculty of Engineering, Majlesi Branch, Islamic Azad University, Esfahan, Iran*
[b]*Department Research Management, Innovation and Commercialization, Universiti Malaysia Kelantan, Kelantan, Malaysia*

An array of air-filled capillary-attached conductive gas sensors was applied to fabricate an electronic nose. The ability of the developed structure was investigated in analyzing the number of components of different gas mixtures. Feature data sets were generated from the dynamic responses of the sensor array to the applied odor database of gas mixtures. Combinations of different feature extraction and classification methods were used to detect the number of components of target gases and validation of each technique was studied. Achievements proved high classification accuracy of the fabricated e-nose in gas mixture component analysis.

(Received September 28, 2015; accepted October 25, 2015)

Keywords: Metal oxide gas sensor, Gas mixture component, Sensor array, Gas diffusion, Electronic nose

1. Introduction

During last three decades the extensive research has been conducted on the development of artificial nose also called electronic nose (e-nose). As a result, this sensing instrument which mimics the mammalian sense of aroma has been commercialized. Numerous applications in a food quality control, medical diagnosis and environmental monitoring have been reported [1]. However, further effort is still needed in order to improve the e-nose performance such as improving the selectivity, and the ability of quantitative analysis in compare with classical instruments such as gas chromatography/mass spectrometry (GC/MS).

The fundamental idea behind the electronic nose is to distinguish different odor samples for certain applications. However, some research and investigations have also reported the ability of the e-nose in analyzing gas mixtures components [2-4]. Researches have investigated the ability of the electronic nose on the gas mixtures analysis by applying the typical structure of e-nose. The typical structure of the electronic nose includes an array of the chemical gas sensors and a pattern recognition unit [1, 5].

This research has focused on the development of the novel structure of the e-nose based on an air-filled capillary attached to a metal oxide semiconductor (MOS) conductometric gas sensor to analyze the number of components in different gas mixtures. The capillary attached Gas Sensor (CGS) based on the diffusion process of gas through the air-filled capillary tube is a simple and efficient approach to improve the performance of the single MOS sensor as well as MOS sensors array employed for e-nose [6, 7].

It has been indicated that the data regarding the nature of a target gas (TG) can easily be extracted from the corresponding transient response of the CGS and any specifically defined point on the transient responses can be applied to compare and detect different gases along with temporal analysis [6, 8, 9].

A laboratory model of the proposed structure has been developed, tested and optimized its performance in vapor mixtures. As a result presented in the next sections, the novel artificial nose employing the transient response is generating high classification rates in quantitative gas mixture analysis, and it will be useful to extend machine olfaction applications.

2. Theory and structure of the CGS

The CGS structure is split into two basic parts: a MOS gas sensor and Quartz air-filled capillary diffusion tube [6]. An image of a fabricated prototype CGS is presented in figure 1. The MOS sensor is either attached or fabricated at the end of a diffusion tube and the attached area is closed and sealed completely. Then, a target gas will solely diffuse from the opposite end of the tube. Equation (1) is generally used to describe the variation of connectivity of the single MOS gas sensor [10-12]. The conductivity variation of the sensing element of a MOS gas sensor, ΔG, to a certain concentration level (C) of a target gas (TG) with specific constants S and m can be delineated as

$$\Delta G = SC^m \tag{1}$$

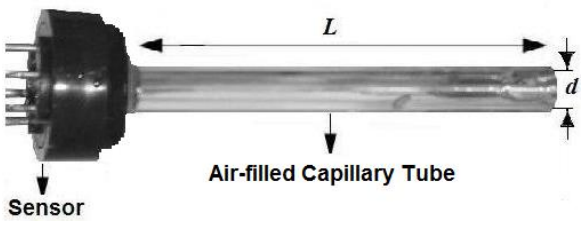

Fig. 1. Picture of a prototype CGS fabricated

The values of S and m determine the respective sensitivity of a sensor provided by the sensor manufacturer. m is also related to the concentration of a TG functionally and the range of this fluctuation is 0.5–0.9 [12]. In an experiment, the diffusion process is started at certain time. The TG has to diffuse through the effective length of the air-filled diffusion tube (L in figure 1) before reaction takes place with the MOS gas sensor. Therefore, the concentration of the TG is time dependent at the closed end of the diffusion tube, where the MOS gas sensor is placed. The dynamic response of the applied MOS gas sensor in the CGS structure is analytically explained by [6]:

$$\Delta G(t) = SC^m(0,t) = 2^m SC_0^m \left[\sum_{n=0}^{\infty}(-1)^n erfc\left(\frac{(2n+1)L}{2\sqrt{Dt}}\right)\right]^m \quad (2)$$

where D is the diffusion coefficient for a TG, L is the effective length of a diffusion tube, and t is the time since the diffusion process started. *erfc(x)* is the complementary error function and x is the real variable:

$$erfc(x) = \frac{2}{\sqrt{\pi}}\int_x^{\infty} e^{-t^2}\,dt \quad (3)$$

Evaluation of equation (2) indicates that a TG with higher D has faster response. Quantitative evaluation of equation (4) can be investigated by comparing any specific defined point on the transient responses of the CGS to different TGs [6].

In this study, a sensor array including 9 CGS prototypes was fabricated. A list of applied MOS gas sensors for fabricating CGS samples is presented in table 1. Quartz tubes of 0.5 mm diameter and 50 mm length were applied to fabricate the CGS samples. These dimensions were selected to optimize selectivity, response time and recovery time due to aim of this study. Longer length and smaller diameter increase the selectivity but make the response time and recovery time longer [13]. However, 0.5 mm diameter was selected to improve the selectivity.

Table 1. List of selected gas sensors to fabricate CGS prototypes.

Sensor No.	Model (Part No.)	Categories	Application
1	SB-15-00	Gas detectors	Propane/butane
2	SB-19-00	Gas detectors	Hydrogen
3	SB-AQ1-04	Indoor air quality	General purpose
4	SP-11-00	Gas detectors	Fuel gas (Hydrocarbons)
5	SP-12A-00	Gas detectors, Fuel cell	Methane
6	SP-19-00	Gas detectors	Hydrogen
7	SP-31-00	Gas detectors	Organic solvents, , Alcohol
8	SP3-AQ2-01	Indoor air quality	General purpose
9	SP3S-AQ2-01	Indoor air quality	General purpose

3. Design of the experiment

3.1. Measurement system

The schematic diagram of the fabricated measurement system is presented in figure 2. The static measurement mode was selected to design and develop the measurement system. In this method the TG has to equilibrate in the measurement environment first [14]. A chamber of 20 liter capacity was selected to build an experiment environment to prepare low level concentrations. A fabricated sensor array was attached to the chamber via an automatic impermeable gate.

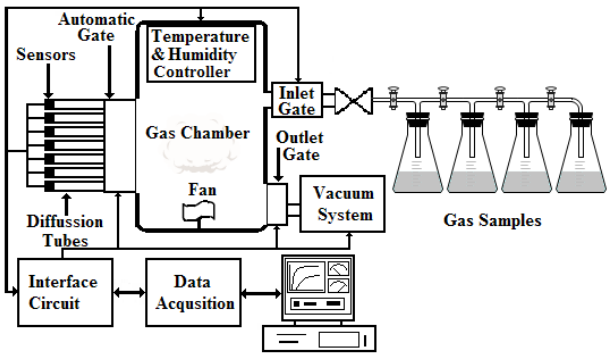

Fig. 2. Schematic diagram of the measurement system designed.

The temperature and humidity of the experiment environment were monitored during all experiments to keep the measurement system under stable conditions and to omit environmental interfering effects from the response of the sensors. The stable environment with constant levels of humidity and temperature provides better reproducibility. Injection of a gas mixture into the chamber was performed when the impermeable gate was closed. The measurement system was paused for a while until the inserted gas mixture settled down completely in the chamber. The impermeable membrane of the gate was removed and measurement was started at $t = 0$.

Diffusion of the equilibrated gas mixture was started through the effective length of the diffusion tubes. The output of sensors was transferred to the digital computer by a data acquisition system. Measurement was continued up to a steady state level and the output converted to the variation of conductivity in time was recorded.

3.2. Odor database

A database of gas mixtures including two to four components of short-chain alcohols was applied to evaluate the classification performance of the fabricated e-nose. Experiment was repeated over different days at different time intervals for each gas mixture to assess the reproducibility of the measurement system. Since experiments were designed in a static mode, gas mixtures were prepared by pumping certain amount of each component into the chamber of the measurement system. A summary of odor databases is presented in tables 2 and 3. Gas mixtures in combinations of the four short-chain alcohols were generated in the different low concentration below 100 ppm. Experiments were repeated over 3 days.

Table 2. Detail of gas mixtures database

Class Label	Odor Type	No. of Gas Mixtures	No. of Experiments per concentration	Total No. of Samples per Gas mixture
1	Mixture of 2	6	9	90
2	Mixture of 3	4	9	90
3	Mixture of 4	1	9	90

Table 3. Detail of gas mixtures identity

Class Label	1	2	3
Class Name	**Mixture of 2 Gases**	**Mixture of 3 Gases**	**Mixture of 4 Gases**
	Methanol &Ethanol	Methanol & Ethanol & 2-Propanol	Methanol & Ethanol & 2-Propanol & 1-Butanol
	Methanol & 2-Propanol	Methanol & Ethanol & 1-Butanol	
	Methanol & 1-Butanol	Methanol & 2-Propanol & 1-Butanol	
	Ethanol & 2-Propanol	Ethanol & 2-Propanol & 1-Butanol	
	Ethanol & 1-Butanol		
	2-Propanol $ 1-Butanol		

3.3. Preprocessing

The flow diagram presented in Fig. 3 describes the processing steps in this study. Signal preprocessing is the first step applied generally to modify the response of sensors and to limit the impact of disturbances. These problems are generated by unequal responses of a sensor and fluctuations due to environmental interfering parameters. Then, features with higher identification impacts could be selected to improve the result of next stages in the pattern recognition and classification process. Any of the following three major categories can be employed in the preprocessing step in any order: baseline manipulation, compression and normalization [15]. Baseline manipulation is employed to reduce the effect of sensor drift. Sensor drift generally causes an unstable response in time with a slow and random variation of the baseline of the response. The manipulation can be based on differential, relative and fractional methods [15-17]. According to the characteristic of the CGS, identification parameters are more related to the original characteristics of the response. Then, preprocessing methods should be

selected keeping the main characteristic of the response untouched. In this study differential baseline manipulation was selected.

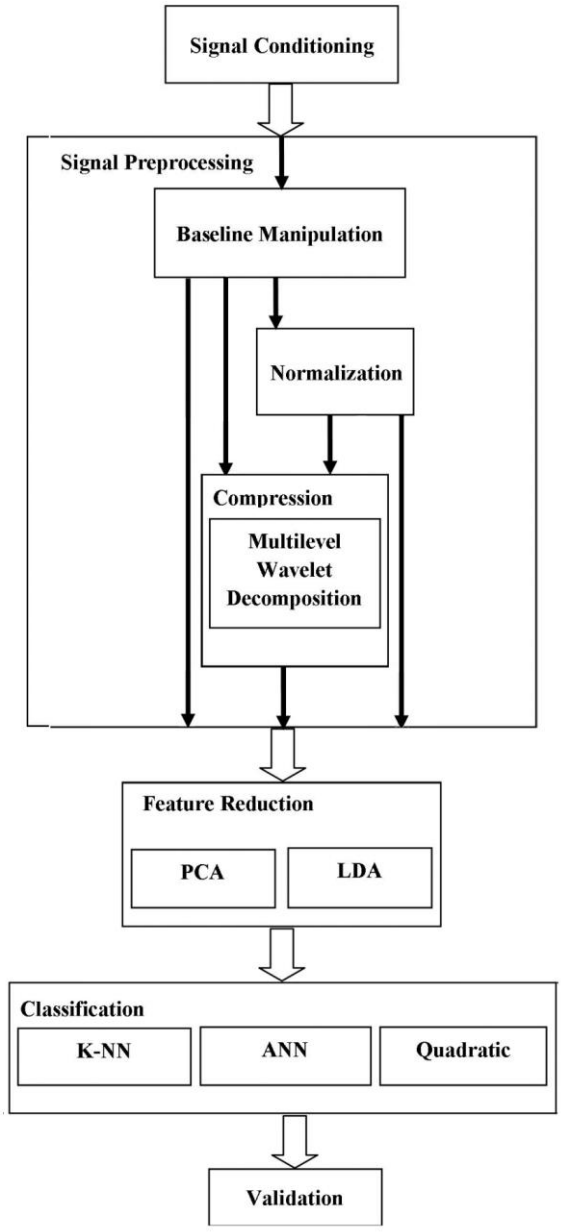

Fig. 3. Flow diagram of processing method applied.

Baseline manipulation is applied in subtracting from each sampling the initial baseline value of transient response:

$$G_m(k) = G_s(k) - G_s(0) \tag{4}$$

where $G_s(k)$ is the original output of the sensor; $G_s(0)$ is the initial baseline output of the sensor and $G_m(k)$ is the adjusted output value of the sensor. The sample of baseline manipulated responses are presented in figure 4.

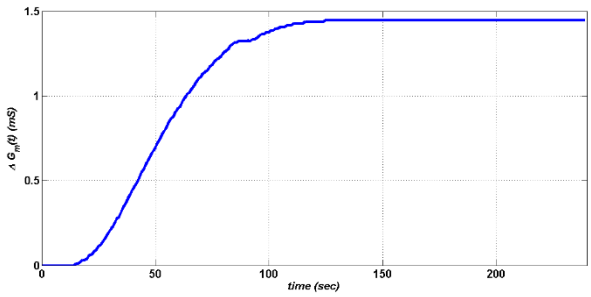

Fig. 4. Response of a CGS to the mixture of methanol and ethanol in 100 ppm after baseline manipulation.

Since previous studies on the CGS were investigated based on analyzing the normalized response of the CGS [6, 8, 9, 13], the second data set was generated from normalized responses. The normalized response of the CGS was generated by using the maximum level of the CGS response in each measurement as a normalization factor:

$$G_n(k) = \frac{G_m(k)}{G_{m\,MAX}} \tag{5}$$

Data compression methods are applied to reduce the number of recorded points per experiment. In this step, different methods can be used, such as sub-sampling, parameter extraction and system identification [18]. Both datasets generated from the baseline manipulated transient responses and normalized responses include a large number of points per sample. This problem can cause the curse of dimensionality and affect the classification process. In the first data set applying the raw signal could also make some disturbances during the identification process. In this study, preprocessing techniques were selected based on minor effects on the original characteristics of the response signal. Multilevel wavelet decomposition could be applied as a suitable option for data compression according to the above conditions. Both mentioned feature data sets were applied to generate other feature data sets based on the output of multilevel wavelet decomposition.

The discrete wavelet transform (DWT) described below was applied to decompose the sensor transient response into multilevel resolution. An overview of the wavelet analysis has been widely described in the literature [19-21]. A brief overview of discrete wavelet decomposition applied in this paper is described as follows.

The classical method of computing the DWT can be implemented by a two channel filter bank [19-21]. The basic idea behind the fast algorithm is to represent the wavelet basis as a set of high-pass and low-pass filters in a filter bank. Following the filtering, the signal is decimated by a factor of 2 [22].

Down sampling by a factor of 2 denotes discarding every other sample of the signal sequence. The outputs of the low pass branch are called wavelet approximation

coefficients, and the outputs of the high-pass branch are called wavelet detail coefficients. The identity of the original signal is stated by the low-frequency component. To decompose an original signal into a multilevel approximation, the high frequency component must be eliminated and the low frequency component must be entered into the next filter bank consecutively. Then, approximation of the original signal can be generated at different levels of resolution by applying multilevel decomposition. The maximum scale can be achieved by performing wavelet decomposition, repetitively. The maximum scale is dependent on the signal length and the wavelet basis length [22].

The main advantage of the multilevel decomposition in representation of the sensor response is the possibility of saving the general attributes of the original signal when the number of features of the sensor response is reduced.

According to classification results, features generated by the Daubechies (db2) wavelet family were presented as the best performance in classification among different wavelet families that were selected and applied. To extract the features from the transient response of the sensor array, the best level of decomposition was selected by trial and error. Finally, four data sets were generated for every odor database including features presented in table 4.

Table 4. Evaluation results of feature extraction and classification methods applied to classify features generated from the sensor array responses to gas mixtures database

Odor Database	Type of Feature	KNN		ANN		Quadratic	
		% Classification Rate		% Classification Rate		% Classification Rate	
		PCA	LDA	PCA	LDA	PCA	LDA
Alcohol Mixture	Baseline manipulated	80.22	94.22	80.54	97.99	50.88	97.77
	Baseline manipulated (DWT)	79.33	99.11	81.82	98.88	49.55	100
	Normalized Response	73.77	74.66	66.81	81.77	44	67.33
	Normalized Response (DWT)	75.77	98.22	70.40	97.99	46.88	98.22

3.4. Feature extraction and classification

Feature selection and feature extraction techniques are generally employed to reduce the curse of dimensionality. Therefore, classification performance and efficiency are improved as well as ease of interpretation and modeling [23, 24]. In the gas identification system and machine olfaction area, principal component analysis (PCA) and linear discriminant analysis (LDA) are mostly of interest among diverse feature extraction and selection methods [17, 18]. PCA is a kind of signal representation method which projects in such a way that maximizes variance directions. The directions are defined based on the first eigenvectors related to the largest eigenvalues of the covariance matrix of input features, where the covariance of input features $\sum_G$ is

$$\sum_G = E[(G-\mu)^T (G-\mu)] \tag{7}$$

where μ is the means vector of features vectors G.

LDA is a supervised signal classification method to maximize class compactness in a direct way and to maximize separation between samples from compact bunches and different bunches. The first eigenvectors of the multiplication result of the within-class covariance inverse matrix and between-class covariance matrices are applied to make projections. The following definition can be applied to describe LDA when a linear projection (W) maximizes the objective function below [15, 17, 25, 26]:

$$J(W) = \frac{W^T \sum_B W}{W^T \sum_W W} \tag{8}$$

where Σ_B is the between-class covariance matrix, and Σ_W is the within-class covariance matrix.

PCA and LDA are employed along with different classifiers to investigate the ability of a gas detection system.

Either two- or three-dimensional projection of the extracted features by PCA and LDA is applied to illustrate the separability between classes, and the compactness of features from the same class and variance of the features from different classes, respectively [17, 18]. PCA and LDA techniques were applied to extract features for all feature data sets. Extracted features by PCA and LDA were applied for gas classification in combination of different classifiers to investigate the abilities of the developed e-nose structure in gas identification and selection of an optimum approach.

The *k*-nearest neighbor (k-NN) classifier, multilayer perceptron (MLP) classifier and the quadratic classifier are well-known methods in the area of gas classification [17, 18]. These classifiers were applied in this study to classify the features extracted by PCA and LDA from feature data sets. In the k-NN classifier *k*-nearest samples in the feature data set are selected to classify unlabeled data. The class with maximum members between *k*-nearest neighbors is assigned as the class number for the unlabeled feature [15, 25, 26]. To provide the highest classification rate, the number of nearest neighbors (k) was selected 3 by trial and

error. Distances were calculated based on the Euclidean distance for this classifier.

MLP is the multilayer feed-forward neural network that includes simple processing elements or neurons. The result of this structure is a complex nonlinear regression. A gradient descent method, which is called back propagation (BP) of errors, is generally applied to train the regression by adjusting the weights of elements of the network [17, 24, 27]. A 3–7–3 layer structure (three inputs, seven neurons in one hidden layer and *three* outputs) was selected for MLP neural network classifier. The number of neurons in the output layer equals the number of classes in the odor database. The network was trained by the Levenberg–Marquardt (LM) optimization algorithm [17].

As the simplest approach, the quadratic classifier approximates the largest posterior probability by assuming unimodal Gaussian density as a likelihood function for each class. In this classifier, decision boundaries between classes are quadratic hyper surfaces [17, 25].

Finally, *N*-fold cross validation was used to estimate the prediction error [17, 26, 28]. This method applied by dividing the feature data set into *N* subsets. *N*−1 subsets are used as the training data set, and the remaining subset is employed as the testing data set. The classification rate is presented by the average value across *N* trials of the testing data sets. Fivefold cross validation ($N = 5$) was used to evaluate the prediction accuracy of each classifier.

4. Results and discussion

Four generated feature datasets for each odor database were applied to PCA and LDA feature reduction techniques and the generated outputs were classified by the mentioned classification approaches. The results of classification performances are presented as follows.

Two-dimensional projection of PCA and LDA outputs to feature data sets of baseline manipulated responses (BMR), wavelet decomposition of baseline manipulated responses (WD-BMR), normalized responses (NR), and wavelet decomposition of normalized responses (WD-NR) generated from the gas mixture odor database are presented in figures 5 and 6, respectively.

The projections well presented the separation of the classes from each other. However, LDA results surpassed the PCA, as expected. For LDA results, projections of extracted features based on WD-BMR indicate higher separability between classes than others. The best within-group compactness was also presented by LDA projection of extracted features from WD-BMR. The impact of wavelet decomposition on between-class separability can be observed by comparing projections in Figs. 5 and 6. The best compactness within the class and separability between classes could be observed in the output of PCA and LDA to WD-BMR (Fig. 5).

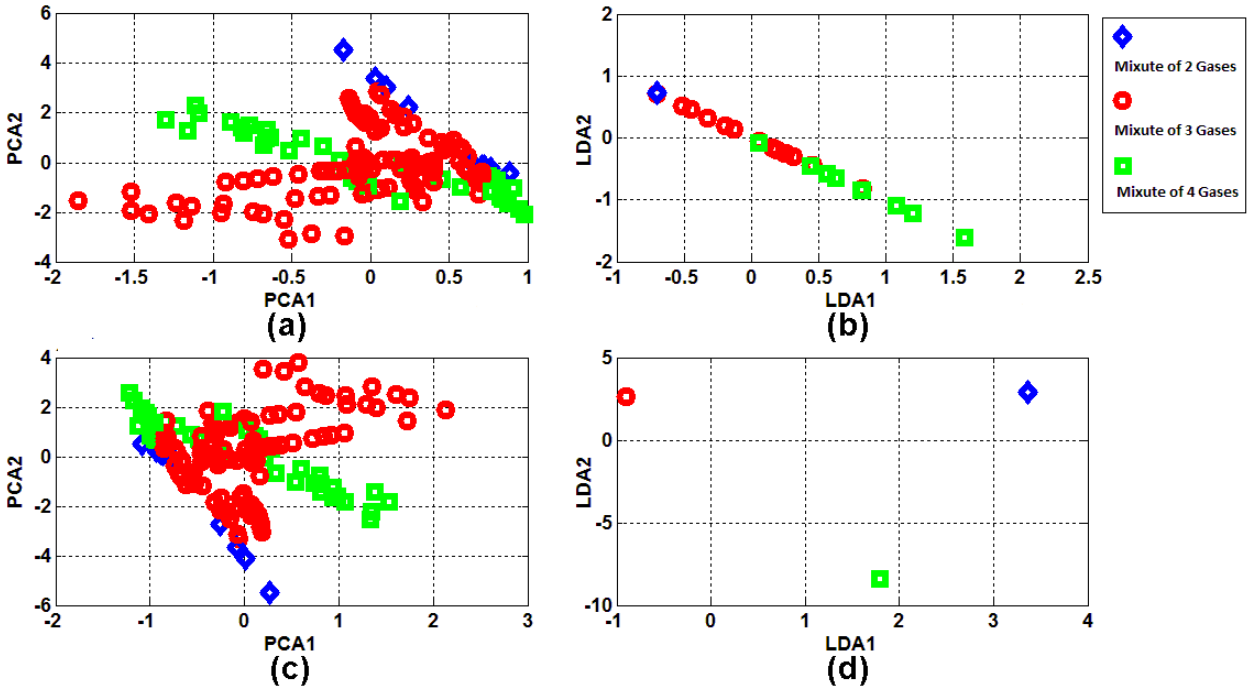

Fig. 5. (a) 2-Dimensional projection of extracted features from the BMR to alcohol mixtures database by PCA. (b) The same using LDA. (c) 2-Dimensional projection of extracted features from the WD-BMR to alcohol mixtures database by PCA. (d) The same using LDA.

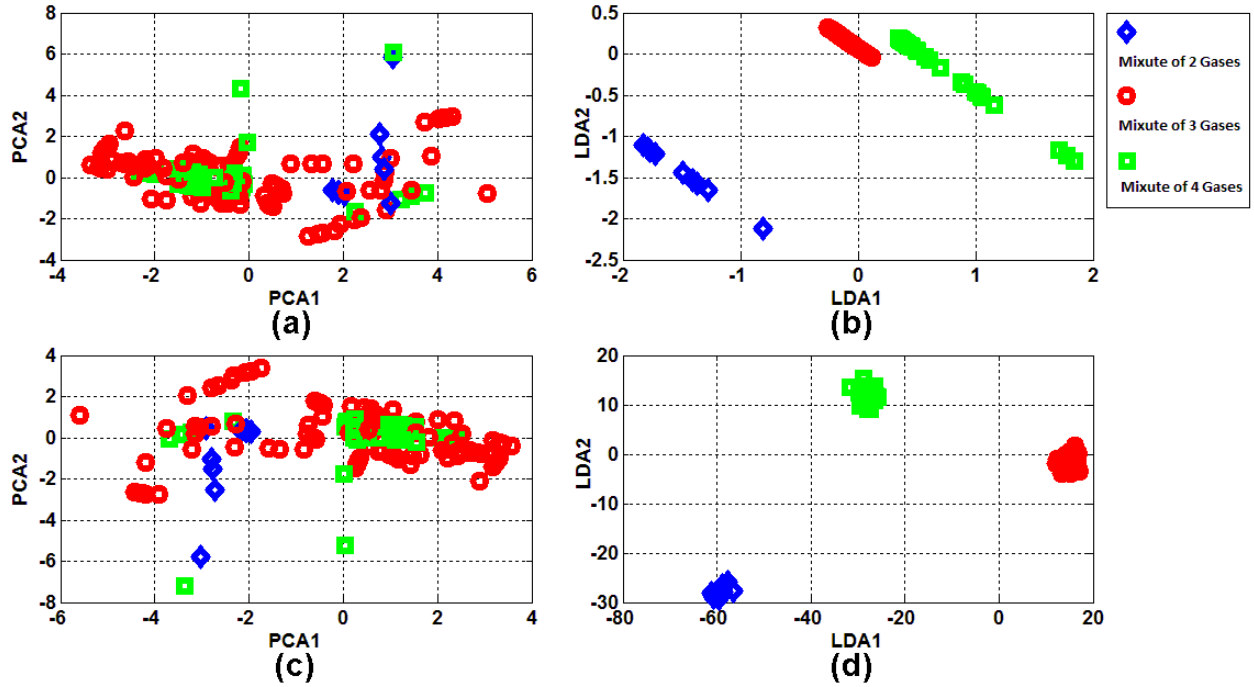

Fig. 6. (a) 2-Dimensional projection of extracted features from NR to alcohol mixtures database by PCA. (b) The same using LDA. (c) 2-Dimensional projection of extracted features from the WD-NR to alcohol mixtures database by PCA. (d) The same using LDA.

The classification results of the alcohol mixtures are shown in table 4. For these data, high classification rate could be obtained using WD-BMR and WD-NR feature data sets. The best classification rates were reported by the classification of LDA output of WD-BMR for all classifiers.

As demonstrated in table 4, achieving a high classification rate based on the developed structure of the e-nose by applying capillary-attached CGSs is possible. However, it depends on not only the classification method but also the type of extracted features and reduction techniques. According to the presented results, extracted features from a baseline manipulated transient response of the sensor array provided the best classification rates. It was also presented that applying multilevel wavelet decomposition improved the classification rates based on transient response analysis.

According to the achieved results, it can be concluded that analysis the number of gas mixture components by the suggested e-nose structure is possible. However, more investigations are required to achieve a perfect instrument.

5. Conclusions

A developed e-nose structure based on the array of capillary-attached gas sensors was designed and fabricated. The identification ability of the developed e-nose structure was investigated by applying gas mixtures database containing short-chain alcohols mixtures. Diverse feature data sets were generated by extracting features from the transient response of the fabricated sensor array to odor database. Different feature extraction and classification techniques were applied to feature data sets, and classification performances were evaluated. Evaluated results indicated high accuracy in classification performance of the developed structure for most of the generated features. The results based on feature data sets generated from the transient response of the sensor array proved that additional identification parameters related to the diffusion properties of odors improved the gas identification process. According to the presented results, feature data set extracted from transient responses of the sensor array along with wavelet decomposition was selected as an optimum feature data set for gas identification. Suggested feature data set illustrated perfect identification performance. Evaluated results based on the above-mentioned procedure also indicated the ability of the developed e-nose structure in gas mixture analysis.

References

[1] T. C. Pearce, S. S. Schiffman, H. T. Nagle, J. W. Gardner, Handbook of Machine Olfaction: Electronic Nose Technology, Wiley-VCH, Weinheim, Germany, 2002.

[2] T. Nakamoto, Y. Nakahira, H. Hiramatsu, T. Moriizumi, , Sensors and Actuators B: Chemical, **76**, 465 (2001).

[3] A. Fort, N. MacHetti, S. Rocchi, B. Serrano, L. Tondi, N. Ulivieri, V. Vignoli, G. Sberveglieri, IEEE Transactions on Instrumentation and Measurement, **52**, 921 (2003).

[4] E. Phaisangittisagul, H.T. Nagle, Sensors and Actuators B: Chemical, **155**, 473 (2011).

[5] K. Arshak, G. Lyons, L. Cavanagh, S. Clifford, Sensor Review, **23,** 230 (2003).
[6] F. Hossein-Babaei, M. Orvatinia, Sensors and Actuators, B: Chemical, **96**, 298 (2003) -303.
[7] B. Bahraminejad, S. Basri, M. Isa, Z. Hambali, Application of the sensor array based on capillary-attached conductive gas sensors for gas detection, measurement science and technology, **21**, 085204 (2010).
[8] F. Hossein-Babaei, M. Hemmati, M. Dehmobed, Sensors and Actuators, B: Chemical, **107**, 461 (2005).
[9] B. Bahraminejad, S. Basri, Z. Hambali, M. Isa, IEICE electronics express, **6,** 876 (2009).
[10] M.A. El Khakani, R. Dolbec, A.M. Serventi, M.C. Horrillo, M. Trudeau, R.G. Saint-Jacques, D.G. Rickerby, I. Sayago, P, Sensors and Actuators, B: Chemical, **77**, 383 (2001).
[11] S.W. Lee, P.P. Tsai, H. Chen, Sensors and Actuators, B: Chemical, **67**, 122 (2000).
[12] V.V. Kissine, V.V. Sysoev, S.A. Voroshilov, Sensors and Actuators, B: Chemical, **79,** 163 (2001).
[13] B. Bahraminejad, S. Basri, Z. Hambali, M. Isa, Measurement Science and Technology, **21**, 065202 (2010).
[14] B.G. Kermani, S.S. Schiffman, H. Troy Nagle, IEEE Transactions on Biomedical Engineering, **46,** 429 (1999).
[15] R. Gutierrez-Osuna, H.T. Nagle, IEEE Transactions on Systems, Man, and Cybernetics, Part B: Cybernetics, **29,** 626 (1999).
[16] R. Gutierrez-Osuna, H.T. Nagle, B. Kermani, S.S. Schiffman, Signal conditioning and pre-processing, in: T.C. Pearce, S.S. Schiffman, H.T. Nagle, J.W. Gardner (Eds.) Handbook of Machine Olfaction: Electronic Nose Technology, Wiley-VCH, Weinheim, Germany, 2002, pp. 105-132.
[17] R. Gutierrez-Osuna, IEEE Sensors Journal, **2**, 189 (2002).
[18] E.L. Hines, P. Boilot, J.W. Gardner, M.A. Gongora, Pattern Analysis for Electronic Noses, in: T.C. Pearce, S.S. Schiffman, H.T. Nagle, J.W. Gardner (Eds.) Handbook of Machine Olfaction: Electronic Nose Technology, Wiley-VCH, Weinheim, Germany, 2002, pp. 133-160.
[19] C.S. Burrus, R.A. Gopinath, H. Guo, Introduction to Wavelets and Wavelet Transforms: A Primer, Prentice-Hall, Englewood Cliffs, NJ, 1998.
[20] M. Vetterli, J. Kovacevic, Wavelets and subband coding, Prentice-Hall, Englewood Cliffs, NJ, 1995.
[21] S. Mallat, A wavelet tour of signal processing, 2nd ed., Academic, San Diego, CA, 1998.
[22] L.M. Bruce, l.H. Koger, J. Li, IEEE Transaction on Geoscience and Remote Sensing, **40**, 2331 (2002).
[23] R.E. Bellman, Adaptive control processes: a guided tour, Princeton University Press, Princeton, New Jersey, 1961.
[24] C.M. Bishop, Neural Networks for Pattern Recognition, Oxford University, New York, 1995.
[25] R.O. Duda, P.E. Hart, D.G. Stork, Pattern classification, 2nd ed., Wiley, New York, 2000.
[26] T. Hastie, R. Tibshirani, J. Friedman, The elements of statistical learning: data mining, inference, and prediction, Springer, New York, 2001.
[27] H. Demuth, M. Beale, Neural network toolbox user's guide: for use with matlab, ver. 4, MathWorks, MA, 2004.
[28] A.K. Jain, R.P.W. Duin, J. Mao, Statistical pattern recognition: A review, IEEE Transactions on Pattern Analysis and Machine Intelligence, **22**, 4 (2000).

*Corresponding author: b.bahraminejad@iaumajlesi.ac.ir